

Understanding the Role of Mitochondria Distribution in Calcium Dynamics and Secretion in Bovine Chromaffin Cells

Amparo Gil, Virginia González-Vélez, José Villanueva and Luis M. Gutiérrez

Abstract Adrenomedullary chromaffin cells are widely used as a valuable model to study calcium-induced exocytosis of dense vesicles. Functional studies demonstrated the important role of organelles in shaping calcium signals in this cell type. Therefore, the study of mitochondria distribution in relation with exocytotic sites is relevant to understand the nature of such modulation. In this paper, we discuss the spatial distribution of mitochondria in bovine chromaffin cells in culture inferred from experimental observations and use a theoretical model for understanding the role played by these organelles in the fine tuning of calcium signals and the modulation of secretion.

1 Introduction

It is well known the key role that calcium plays as messenger in a large number of vital processes, such as secretion of hormones and neurotransmitters, muscle contraction and genetic transcription, among others [1, 20]. Regarding the release of neurotransmitters, the vast majority of synapses in the central nervous system are chemical, as are all synapses between nerves and muscles. When an action

A. Gil (✉)

Depto. de Matemática Aplicada Y CC de la Comput, Universidad de Cantabria,
39005 Santander, Spain
e-mail: amparo.gil@unican.es

V. González-Vélez

Area de Química Aplicada, Universidad Autónoma Metropolitana-Azcapotzalco,
02200 Mexico city, Mexico
e-mail: vgv@correo.azc.uam.mx

J. Villanueva · L.M. Gutiérrez

Instituto de Neurociencias, Centro Mixto Universidad Miguel Hernández-CSIC,
Sant Joan d'Alacant, Alicante, Spain
e-mail: jvillanueva@umh.es

L.M. Gutiérrez

e-mail: luisguti@umh.es

potential invades the terminal, the depolarization opens voltage-sensitive calcium channels, allowing calcium ions to enter the nerve terminal and trigger the transmitter release process. This model, established by Katz and Miledi [10, 11] for the release of neurotransmitter in the frog neuromuscular junction, has been extended to release processes in neurons, neuroendocrine and endocrine cells and many other cell types.

In the particular case of chromaffin cells (a type of neuroendocrine cells located in the adrenal glands), the release of catecholamines takes place in response to the elevation of cytosolic calcium in a process involving the transport of granules, translocation to the plasma membrane, docking at the secretory sites, and finally the fusion of membranes with extrusion of soluble contents [2]. Chromaffin cells have been widely used to study neurosecretion since they exhibit similar calcium dependence of several exocytotic steps as synaptic terminals do, but having the great advantage of being larger than neurons that facilitates the experimental study of exocytosis and calcium dynamics. In chromaffin cells, major cellular structures such as the cortical cytoskeleton seem to play fundamental roles in different stages of the secretory cascade [9], whereas organelles such as mitochondria and the endoplasmic reticulum appear to control and shape calcium elevations at the subplasmalemmal region [5]. In connection to this second aspect, a characterization of the populations of mitochondria and ER elements in cultured bovine chromaffin cells in relation with its distance to the secretory apparatus or exocytotic sites, was presented in [18].

In this paper, we discuss experimental findings on the mitochondria distribution in bovine chromaffin cells in culture obtained using confocal fluorescence microscopy and use a theoretical stochastic model for understanding the role played by these organelles in the fine tuning of calcium signals and the modulation of secretion. The modeling approach, which describes the entry through L and P/Q voltage-dependent calcium channels (VDCC), the 3-D diffusion of calcium ions and the kinetic reactions of calcium and buffers, is particularly appropriated for the study of media with an inhomogeneous spatial distribution of obstacles [15], as seems to be the case of mitochondria in chromaffin cells. It should be mentioned that the specific model for mitochondria organelles is not yet perfect and should be further validated using more experimental data and more extensive simulations.

2 Experimental Results

The experimental protocol for characterizing the populations of mitochondria and ER elements in cultured bovine chromaffin cells, was described in detail in [18]. We briefly discuss here the experimental protocol and present two new figures summarizing the experimental findings.

2.1 *Experimental Materials and Methods*

Bovine chromaffin cell isolation and culture chromaffin cells were prepared from bovine adrenal glands by collagenase digestion and separated from the debris and erythrocytes using centrifugation on Percoll gradients as described before [7, 8]. After extensive washing, cells were maintained as monolayer cultures in Dulbecco modified Eagles medium (DMEM) supplemented with 10% fetal calf serum, 10 μm cytosine arabinoside, 10 μm 5-fluoro-2'-deoxyuridine, 50 IU/ml penicillin, and 50 g/ml streptomycin. Finally, cells were harvested at a density of 150,000 cells/cm² in 22 mm diameter coverslips coated with polylysine. Experiments were done in Krebs/HEPES (K/H) basal solution containing 134 mm NaCl, 4.7 mm KCl, 1.2 mm KH₂PO₄, 1.2 mm MgCl₂, 2.5 mm CaCl₂, 11 mm glucose, 0.56 mm ascorbic acid and 15 mm HEPES/Na, pH 7.4. Cells were stimulated for 1 min using a depolarizing solution with 59 mm high potassium (obtained by replacing isosmotically NaCl by KCl) in K/H basal solution. Cells were used between the third and sixth day after plating.

2.1.1 *Visualization of F-Actin Cytoskeleton and Mitochondria by Confocal Fluorescence Microscopy*

Chromaffin cells were transfected with GFP-lifeact, a 17 amino acid peptide binding to F-actin without altering its dynamics in vivo or in vitro studies using the Amaxa basic nucleofector kit for primary mammalian neuronal cells (Amaxa GmbH, Koehl, Germany) as described in [17]. 48 h later, cells were incubated either with 1 μm mito-tracker green (Invitrogen, Eugene, Or, USA) for a 15 min period at room temperature.

Cell fluorescence was studied in an Olympus Fluoview FV300 confocal laser system mounted on a IX-71 inverted microscope incorporating a 100X PLAN-Apo oil-immersion objective with 1.45 n.a. Excitation was achieved using Ar and HeNe visible light lasers. After acquisition, images were processed using the ImageJ program. For the statistical analysis, the nonparametric Mann Whitney test for paired samples or the 1 way ANOVA Kruskal–Wallis test were used. Differences were considered significant when $p < 0.05$. Data are expressed as mean + SEM obtained from experiments performed in a number (n) of individual cells from at least three different cultures.

2.2 *Mitochondria Distribution in Bovine Chromaffin Cells in Culture*

The confocal fluorescence images shown in Fig. 1 evidence two different populations of mitochondria in bovine chromaffin cells in the culture. These populations are represented in distinct green (perinuclear mitochondria) and yellow (cortical mitochondria) in the 3-D reconstruction shown in Fig. 1b. The existence of these two different populations was further supported with the measurements of the green

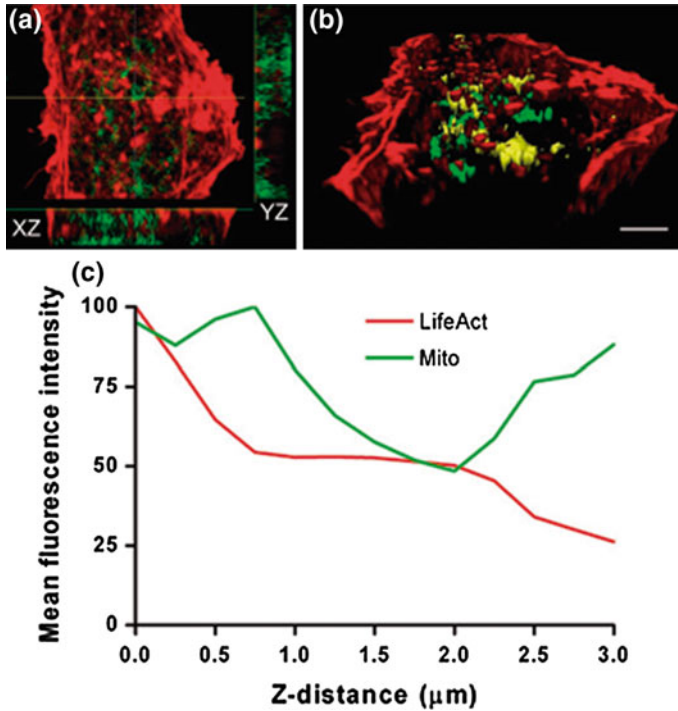


Fig. 1 Confocal microscopy images show two populations of mitochondria in chromaffin cells. Confocal images from representative experiments performed in cultured bovine chromaffin cells expressing RFP- Life Act (*red channel*) and labeled with mitotracker *green*. **a** Confocal planes separated by $0.2\ \mu\text{m}$ from the basal cortical region to the equatorial plane were used to reconstruct cell fluorescence (XY, YZ and XZ planes). The YZ and XZ planes evidenced the low fluorescence layer separating two populations of mitochondria. **b** 3-D image obtained with Imaris showing the perinuclear mitochondria in *green* as well as the cortical mitochondria in *yellow*. **c** Normalized fluorescence for the different confocal planes determined for Life Act fluorescence (*red line*), and mitotracker (*green line*) represented in function of the distance measured from cortical basal to the equatorial plane ($3\ \mu\text{m}$ in total). Bar in **b** represents $3\ \mu\text{m}$

fluorescence intensity in the different confocal planes (Fig. 1c, green line). From these measurements, it is clear the presence of an external population of mitochondria associated with the cortical region ($0\text{--}1\ \mu\text{m}$ of the cell limit) and an internal population around $2\text{--}3\ \mu\text{m}$ of the cell limits.

The experiments also reveal that two subpopulations of cortical mitochondria exist in the vicinity of exocytotic sites: the images shown in Fig. 2a, b were used to measure distances of secretory sites (punctate green dots) to the nearest mitochondria (red elongate forms) and represented in form of distributions. The distance distribution analysis shown in Fig. 2c shows that $\sim 30\%$ of secretory sites colocalized with mitochondria. As can be seen, there is also a significant population of mitochondria around the $300\text{--}500\ \text{nm}$ distance.

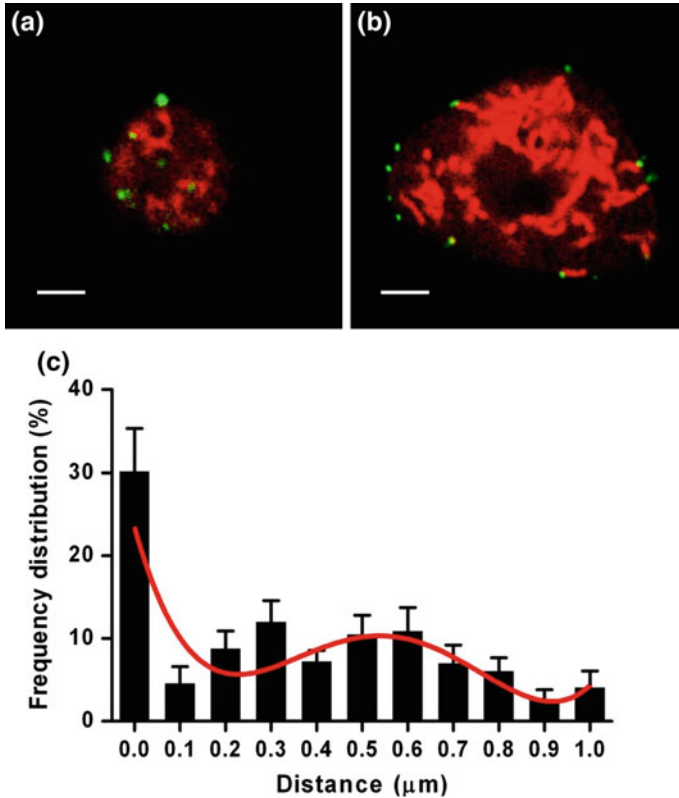


Fig. 2 Cortical mitochondria locate close to the secretory sites. Cultured chromaffin cells incubated with mitotracker red were stimulated during 1 min with a 59 mM KCl solution at room temperature (21–22 C). Secretion was stopped by lowering the temperature using ice-cooled buffer. Secretory sites were labeled using an anti-DβH antibody followed by a secondary antibody coupled to Cy-2 (*green fluorescence*) in ice-cold buffer to prevent endocytosis. The distribution of cortical mitochondria and secretory sites was studied acquiring confocal images of the cortical area in polar sections (a) or equatorial sections (b) to calculate distances between secretory sites and the nearest mitochondria (N = 347 distances from 10 cells). These distances were used to build a distribution using 0.1 μm bin size (c). *Red line* is the best fit to a polynomial function. Bars in a and b represent 3 μm

3 Theoretical Model

The simulation scheme used in this work is an extension of the algorithms developed by the authors [6, 14]. The Monte Carlo algorithm has proved to be successful in the study of the influence of the geometry in the exocytotic response of neuroendocrine cells and presynaptic terminals. For the spatial resolutions that are relevant (of the order of 100 nm in neuroendocrine cells or 10 nm in presynaptic terminals) and the typical concentrations of calcium in chromaffin cells, we can expect few calcium

ions inside each cube of 100nm of side (~ 7 ions for $10\mu\text{m}$) and also a moderate number of calcium binding sites. Then, it seems more appropriate a particle-based approach instead of using a continuous modeling in terms of concentrations.

Our algorithm implements a microscopic simulation in which the fundamental variables are the number of ions and buffers. The average values of the output of our simulation converge to macroscopic simulations when considering symmetrical configurations.

A conical domain is appropriate to describe buffered diffusion in the submembrane domain of spherical cells (which is the case of chromaffin cells in good approximation). The base of the cone represents the membrane of the cell in which voltage-dependent calcium channels are distributed. An orthogonal 3-D regular grid maps the domain of simulation with a distance between grid points Δl . Each point of the grid is associated with a cubic compartment of volume $(\Delta l)^3$. The 3-D diffusion of calcium ions and possible mobile buffers is modeled as a random walk process. The first-order kinetic reactions of calcium ions and buffers are interpreted (and solve) probabilistically.

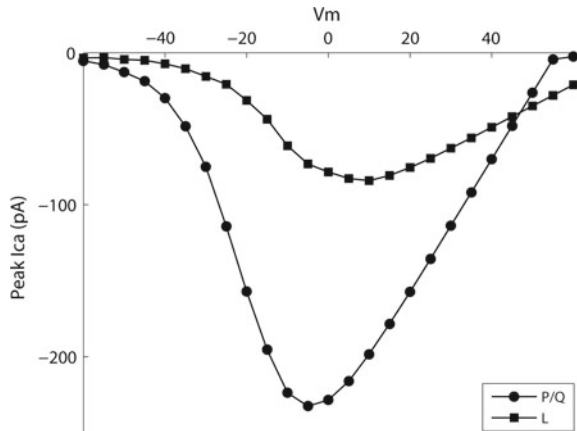
Some of the parameter values used in the model can be found in the Table 1.

To simulate currents through calcium channels, we use a simple stochastic scheme where every channel of the total population may transit from its present state to an open, closed or inactive state in response to voltage and calcium concentrations (the transition parameters between states depend on voltage and local calcium concentrations). Then, the total current is the sum of unitary currents due to open channels; the unitary currents are specific to each channel type and depend on its unitary conductance. In our simulations, we consider that each channel cluster is formed by

Table 1 Parameters used in the simulations

Geometrical parameters	
Radius	$r = 1\mu\text{m}$
Height	$h = 5\mu\text{m}$
Spatial resolution	$\Delta x = 100\text{nm}$
Kinetic parameters	
<i>Calcium</i>	
Basal concentration	$[Ca^{2+}]_0 = 0.1\mu\text{m}$
Diffusion coefficient	$D_{Ca} = 220\mu\text{m}^2/\text{s}$
<i>Endogenous Buffer</i>	
Total concentration	$[B] = 500\mu\text{m}$
Forward binding rate	$k_{on} = 5.10^8\text{m}^{-1}\text{s}^{-1}$
Dissociation constant	$K_D = 10\mu\text{m}$
<i>Secretory vesicles</i>	
Number of binding sites	3
Forward binding rate	$k_{on} = 8.10^6\text{m}^{-1}\text{s}^{-1}$
Dissociation constant	$K_D = 13\mu\text{m}$

Fig. 3 Simulation of calcium entry through P/Q and L-type Ca^{2+} channels in our algorithm: current to voltage relationships considered in the channel gating kinetic schemes



two P/Q- and one L-type calcium channels, according to experimental estimations of channel populations involved in secretion in chromaffin cells [13]. In Fig. 3, the simulated currents to voltage relationships for the L and P/Q calcium channels are shown.

3.1 Modeling Mitochondria as Obstacles for Diffusion of Calcium Ions

In our simulation scheme, mitochondria are modeled as permeable obstacles for diffusion. The distribution of mitochondria inside the simulation domain is made (randomly) according to the experimental findings: (a) 38% of cortical mitochondria (located from 0 to 1 μm to the cellular membrane); (b) 15% of cytoplasmic mitochondria (located from 1 to 2 μm to the cellular membrane); and (c) 47% of internal mitochondria (located from 2 to 3 μm to the cellular membrane). From the cortical mitochondria 1/3 (12.6% of total) are colocalized with calcium channels and 2/3 (25.4% of total) are at 300 nm mean distance. In Fig. 4, we show a representation of the base of the cone used as 3-D simulation domain and its first three slices. Three clusters of voltage-dependent calcium channels (VDCC) and two cortical mitochondria are also shown in the figure. The calcium ions enter through the calcium channels and diffuse inside the cytosol. When in the diffusion process calcium ions are trapped by a compartment corresponding to a mitochondria, the obstructed diffusion inside the mitochondrial matrix is simulated by moving them in exactly the same way that calcium ions are moved in the cytosol, but only after a number N of simulation steps. Although the treatment of diffusion inside mitochondria is simplistic, it has the advantage of using just a single parameter that can be constrained by the available experimental observations.

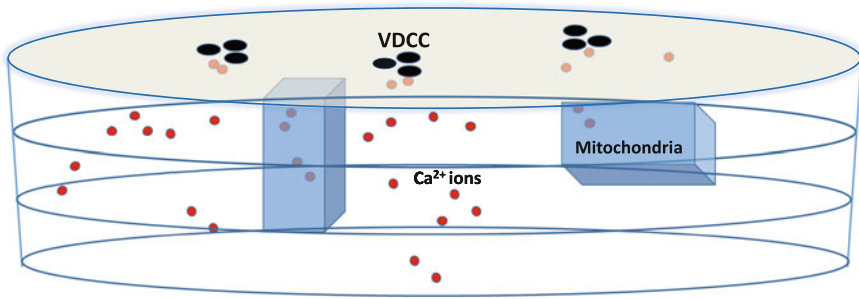


Fig. 4 Schematic representation of the three upper slices of the 3-D simulation domain including three VDCC and two cortical mitochondria

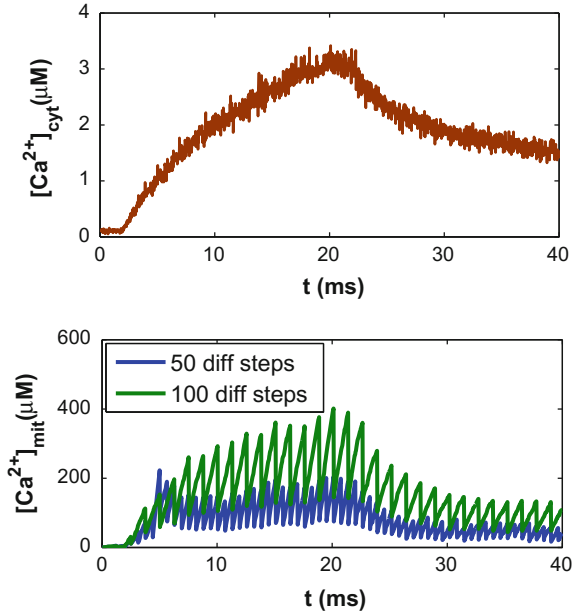
In order to estimate a reasonable value of N in our approach, we have taken into account experimental evidence in chromaffin cells suggesting that: (a) the amount of calcium taken up by the subpopulation of mitochondria in the immediate vicinity of the VDCC could be very large, even as high as $300\text{--}400\ \mu\text{m}$ during maximal stimulation of Ca^{2+} entry through calcium channels [16] and (b) during stimulation, calcium entering through the plasma membrane is taken up preferentially by mitochondria and that there is very little calcium uptake by the endoplasmic reticulum (ER). Therefore, in a first approximation to the problem it seems reasonable to exclude the effect of the ER on the calcium profiles and limit to the study of mitochondria organelles.

Figure 5 (lower figure) shows the average calcium concentration for two different values of N ($N = 50, 100$) inside the compartments corresponding to the cortical mitochondria closest to the VDCC during the simulated stimulus. As can be seen, the calcium fluctuations inside the mitochondria peak at $\sim 200, \sim 400\ \mu\text{m}$ for $N = 50, N = 100$, respectively. Therefore, a value of $N = 100$ for simulating the obstructed diffusion inside the mitochondrial matrix, seems to generate mitochondrial calcium concentrations closer to the experimental observations during the simulated stimulus.

As a comparison, Fig. 5 (upper figure) also shows the average cytoplasmic calcium concentration from 0 to $100\ \text{nm}$ to the cellular membrane. In the computation of the cytoplasmic calcium concentration we have excluded those compartments corresponding to a mitochondria. As can be seen, this average calcium concentration peaks at few micromolar, in contrast to the high calcium levels reached inside the mitochondria matrix. These findings are in agreement with the idea that mitochondria may act as a spatial buffer in many cells, regulating the local Ca^{2+} concentration in cellular microdomains [3] and stopping the progression of the calcium ions toward the cell core [5].

In our study, we have also computed the possible impact of the mitochondria calcium uptake on the secretory response of chromaffin cells using a standard kinetic model for the secretory sensor of vesicles in this cell type [12]. The kinetic model is a noncooperative kinetic scheme in which three calcium ions have to bind to a protein to achieve vesicle fusion. In the simulation scheme, secretory vesicles are considered

Fig. 5 Calcium concentrations in the submembrane domain. *Upper figure* average cytoplasmic calcium concentration from 0 to 100 nm to the cellular membrane. *Lower figure* average calcium concentrations inside the compartments corresponding to the cortical mitochondria closest to the VDCC. Two different values of the retarded diffusion steps ($N = 50, 100$) are considered in the calculations for comparison

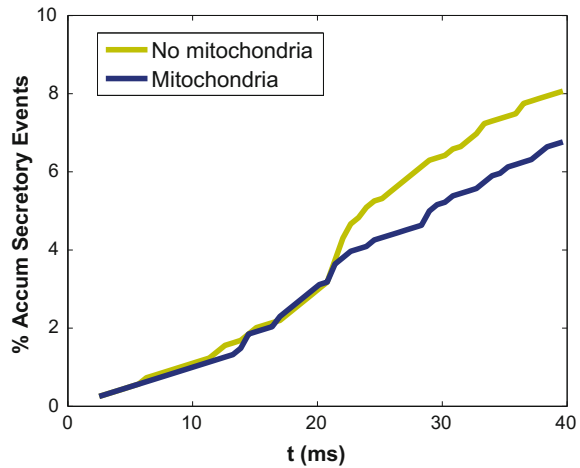


as additional buffers in the medium. These vesicles are assumed to represent the readily releasable pool of vesicles (RRP) [19]. Different distances of vesicles in this pool from the VDCC were simulated by considering few hundreds of random configurations in the first slice of the simulation domain.

In Fig. 6, we show the comparison of the percentage of the accumulated number of vesicles that have fused to the membrane when mitochondria are considered or not in the medium. It is important to note, that the accumulated secretion time course shown is the average of the results obtained with the hundreds of random distances of vesicles from the VDCC mentioned before, not a particular simulation result. As can be seen, the presence of mitochondria moderates the secretory response of the RRP after the calcium peak of the simulated stimulus, in agreement with the idea that mitochondria could play a significant role in the modulation of secretion in chromaffin cells [4].

Future work will involve the refinement of the model for mitochondria organelles in chromaffin cells and other cell types: the model should be further validated using more experimental data and more extensive simulations. Also, the predictive power of the model should be studied. It will be also interesting to include the effect of the Ca^{2+} -induced Ca^{2+} release (CICR) mechanism from the endoplasmic reticulum (excluded in the present study). Modeling this process, along with the entry of calcium through calcium channels and the mitochondria calcium uptake, will allow us to obtain a more clear perspective of the functional triad controlling exocytosis in chromaffin cells.

Fig. 6 Percentage of the accumulated number of vesicles that have fused to the membrane when mitochondria are considered or not in the medium. The accumulated secretion time course shown is the average of the results obtained with few hundreds of random distances of vesicles from the VDCC



Acknowledgements This study was supported by grants from the Spanish Ministerio de Economía y Competitividad (BFU2011-25095 to LMG).

References

1. Augustine, G.J. How does calcium trigger neurotransmitter release?. *Curr Opin Neurobiol.* 11:320–326 (2001)
2. Burgoyne, R.D., Morgan, A., Robinson, I., Pender, N., Cheek, T.R. Exocytosis in adrenal chromaffin cells. *J. Anat.* 183 (Pt 2):309–314 (1993)
3. Duchen, M.R. Mitochondria and calcium: from cell signalling to cell death. *J. Physiol.* 529.1: 5768 (2000)
4. García, A.G., García-De-Diego, A.M., Gandía, L., Borges, R., García-Sancho, J. Calcium signaling and exocytosis in adrenal chromaffin cells. *Physiol Rev.* 86(4):1093–131 (2006)
5. Garcia-Sancho, J., de Diego, A.M., Garcia, A.G. Mitochondria and chromaffin cell function. *Pflugers Arch.* 464:33–41 (2012)
6. Gil, A., Segura, J., Pertusa, J.A.G., Soria, B. Monte Carlo Simulation of 3-D Buffered Ca²⁺ Diffusions in Neuroendocrine Cells. *Biophys. J.* 78(1): 13–33 (2000)
7. Gil, A., Gutierrez, L. M., Carrasco-Serrano, C., Alonso, M. T., Viniestra, S. and Criado, M. Modifications in the C terminus of the synaptosome associated protein of 25 kDa (SNAP-25) and in the complementary region of synaptobrevin affect the final steps of exocytosis. *J. Biol. Chem.* 277: 9904–9910 (2002)
8. Gutierrez, L. M., Ballesta, J. J., Hidalgo, M. J., Gandia, L., Garcia, A. G. and Reig, J. A. A two-dimensional electrophoresis study of phosphorylation and dephosphorylation of chromaffin cell proteins in response to a secretory stimulus. *J. Neurochem.* 51: 1023–1030 (1988)
9. Gutierrez, L.M. New insights into the role of the cortical cytoskeleton in exocytosis from neuroendocrine cells. *Int. Rev. Cell Mol. Biol.* 295:109–137 (2012)
10. Katz, B., Miledi, R. The effect of calcium on acetylcholine release from motor nerve terminals. *Proc. R. Soc. London B* 161: 496503 (1965)
11. Katz, B., Miledi, R. The timing of calcium action during neuromuscular transmission *J. Physiol. (London)* 189: 535544 (1967)

12. Klingauf, J., E. Neher. Modeling buffered Ca^{2+} diffusion near the membrane: implications for secretion in neuroendocrine cells. *Biophys. J.* 72:674–690 (1997)
13. Lukyanetz, E.A., Neher, E. Different types of calcium channels and secretion from bovine chromaffin cells. *Eur. J. Neurosci.* 11: 2865–2873 (1999)
14. Segura, J., Gil, A., Soria, B. *Biophys. J.* Modeling study of exocytosis in neuroendocrine cells: influence of the geometrical parameters. 79(4): 1771–1786 (2000)
15. Vilaseca, E., Pastor, I., Isvoran, A., Madurga, S., Garcés, J.L., Mas, F. Diffusion in macromolecular crowded media: Monte Carlo simulation of obstructed diffusion vs. FRAP experiments. *Theor. Chem. Acc.* 128, Issue 4–6: 795–805 (2011)
16. Villalobos, C., Nunez, L., Montero, M., García, A.G., Alonso, M.T., Chamero, P., Alvarez, J., García-Sancho, J. Redistribution of Ca^{2+} among cytosol and organella during stimulation of bovine chromaffin cells. *FASEB J* 16:343–353 (2002)
17. Villanueva, J., Torres, V., Torregrosa-Hetland, C. J., Garcia-Martinez, V., Lopez- Font, I., Viniegra, S. and Gutierrez, L. M. F-Actin-Myosin II Inhibitors Affect Chromaffin Granule Plasma Membrane Distance and Fusion Kinetics by Retraction of the Cytoskeletal Cortex. *J. Mol. Neurosci.* 48: 328–338 (2012)
18. Villanueva, J., Viniegra, S., Giménez-Molina, Y., García-Martínez, V., Expósito-Romero, G., del Mar Frances, M., García-Sancho, J., Gutiérrez, L.M. The position of mitochondria and ER in relation to that of the secretory sites in chromaffin cells. *J Cell Sci.* 127(23), 5105–14 (2014)
19. Voets, T., Neher, E., Moser, T. Mechanisms underlying phasic and sustained secretion in chromaffin cells from mouse adrenal slices *Neuron* (23): 607–615 (1999)
20. Whitfield, J.F., Chakravarthy, B.: *Calcium: The Grand-Master Cell Signaler*. NRC Research, Ottawa (2001)